On the Assessment of Through-Wall Circumferential Cracks in Steam Generator Tubes With Tube Supports

Xin Wang
Mem. ASME
Department of Mechanical and Aerospace Engineering,
Carleton University,
Ottawa, Ontario K1S 5B6, Canada

Wolf Reinhardt
Mem. ASME
Nuclear Engineering,
Babcock & Wilcox Canada,
Cambridge, Ontario N1R 5V3, Canada

The assessment of steam generator tubes with defects is of great importance for the life extension of steam generators. Circumferential through-wall cracks are the most severe of all tube circumferential defects, and usually require plugging of the affected tubes. The assessment of the tubes with through-wall circumferential cracks or cracks projected to become through-wall can be conducted using the failure assessment diagram (FAD) approach. This approach requires the calculation of the stress intensity factor and the limit load. The available stress intensity factor and limit load solutions for cracked tubes do not include the constraining effect of the tube supports. In the present paper, it is shown that this can be overly conservative. Solutions for stress intensity factors and limit loads are presented for tubes with circumferential through-wall cracks including the effect from the tube support plates. Different values of support spacing are considered. Based on these solutions, the assessment of a typical steam generator tube is demonstrated.
[DOI: 10.1115/1.1511737]

1 Introduction

The assessment of steam generator tubes with defects is of great importance for the life extension of the nuclear steam generators. Circumferential through-wall cracks are the most severe defects of all tube circumferential indications, and usually they directly result in the plugging of the tubes. If it is suspected that a detected crack might become through-wall before the next plant outage, it is critical that the safe operation of this tube can be demonstrated (safety against rupture). The U.S. Nuclear Regulatory Commission (NRC) requires an evaluation of all detected defects for the affected steam generator tubes to remain in service [1].

The assessment of the tubes with through-wall circumferential cracks can be conducted using the failure assessment diagram (FAD) approach [2,3]. The knowledge of the stress intensity factor and the limit load for the tubes with the appropriate boundary conditions are necessary to perform a FAD analysis.

The tube axial load under both normal service and accident conditions controls the failure of steam generator tubes with circumferential cracks. When a free tube as shown in Fig. 1(a) is subjected to an axial tensile stress, rotation at the ends will occur due to the unsymmetrical partial circumferential crack. However, the tubes in a steam generator are supported at periodic intervals and the rotations at the ends of a single span are constrained. This constraint will cause a compressive bending stress at the crack tip compared to the unsupported tube. The bending stress will help the tube to sustain a larger size crack. Experimental results showing this effect have been documented by EPRI [4].

The available stress intensity factor and limit load solutions for cracked tubes do not include the effect of the tube supports (as shown in Fig. 1(a)). The direct use of those solutions will result in overly conservative failure predictions. In the present paper, stress intensity factor and limit load solutions are presented for a tube with a circumferential through-wall crack including the restraint effect from the tube support plates. Different values of spacing of the span are considered. The crack is assumed to be located at midspan, which is a conservative assumption because it minimizes the constraint that the support plates exercise. Based on the obtained solutions, the assessment of a typical steam generator tube with through-wall partial circumferential cracks supported by support plates is demonstrated.

Contributed by the Pressure Vessels and Piping Division and presented at the Pressure Vessels and Piping Conference, Atlanta, Georgia, July 22–26, 2001, of THE AMERICAN SOCIETY OF MECHANICAL ENGINEERS. Manuscript received by the PVP Division, November 8, 2001; revised manuscript received July 30, 2002. Associate Editor: S. Y. Zamrik.

2 Equivalent Cantilever Beam

In the real steam generators, support plates support the tube at regular intervals. Each support plate can be thought of as simple support of the beam that represents the cracked tube. That is, the support restricts the transverse displacement, but not the rotation of the tube. A rotational constraint on the tube is created due to the presence of several supports. When there are about three supports on either side of the cracked span, the tube behaves like a periodically supported beam of infinite length. For convenience, the effect of the rotational constraint on the cracked span can be modeled using a cantilever beam with zero rotation at its end on each side of the crack as in Fig. 1(b). If the span between any two supports is L_{real}, then the L (equivalent length of the cantilever) that must be used for zero rotation at the end is found using the method demonstrated in Appendix B. The equivalent beam length L used in the zero rotation model is found to be

$$L = 1.58 L_{\text{real}} \tag{1}$$

Appendix B gives details of the derivation.

3 Stress Intensity Factor Solution

In order to include the effect of the bending constraint into the stress intensity factor, for a given crack size and a tensile stress σ_t, the corresponding bending stress is calculated first. Then the stress intensity factor can be obtained using superposition of the tensile and bending load cases. The bending stress can be calculated by a compliance analysis for the cracked tube. This method was documented by Marchand et al. [5] using the example of an edge cracked plate. It is applied to a tube with a single through-wall circumferential crack in the present analysis.

Compliance Analysis Method. For the cracked tube with support plate modeled as shown in Fig. 1(b), the reaction bending moments at the ends can be calculated by a compliance analysis

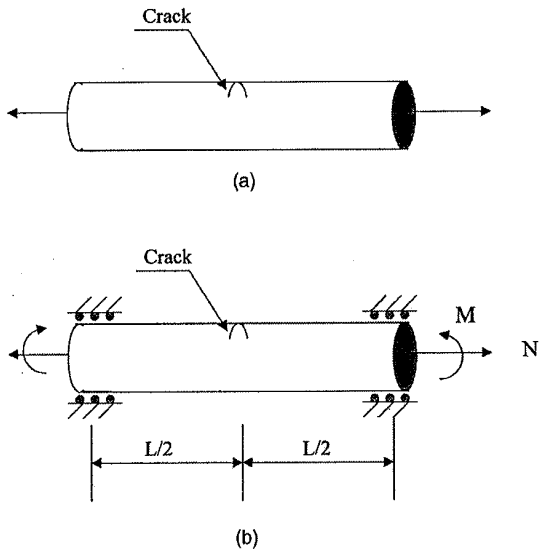

Fig. 1 Tubes with and without tube support plates—(*a*) without tube support plates, (*b*) with tube support plates

method as summarized by Marchand et al. [5]. For a general cracked tube as shown in Fig. 2, the axial displacement δ and rotation θ of the tube at the support location can be obtained from the summation of "cracked" and "uncracked" components

$$\begin{pmatrix} \delta_{\text{total}} \\ \theta_{\text{total}} \end{pmatrix} = \begin{pmatrix} \delta_c \\ \theta_c \end{pmatrix} + \begin{pmatrix} \delta_{nc} \\ \theta_{nc} \end{pmatrix} \tag{2}$$

where the index c relates to the contribution of the crack, and nc denotes the tube without crack. The compliance relating the force and displacement of the uncracked tube has the standard solution:

$$\begin{pmatrix} \delta_{nc} \\ \theta_{nc} \end{pmatrix} = \begin{bmatrix} L/EA & 0 \\ 0 & L/EI \end{bmatrix} \begin{pmatrix} N \\ M \end{pmatrix} \tag{3}$$

In Eq. (3), N stands for the axial tube force, and M for the bending moment; E is Young's modulus, A and I are area and moment of inertia for the uncracked tube cross section, respectively. The compliance for the crack is obtained by considering the complementary energy of the specimen, U, in terms of N and M

$$U(N,M) = \frac{1}{2}[N \quad M]\left(\begin{bmatrix} \delta_c \\ \theta_c \end{bmatrix} + \begin{bmatrix} \delta_{nc} \\ \theta_{nc} \end{bmatrix} \right) \tag{4}$$

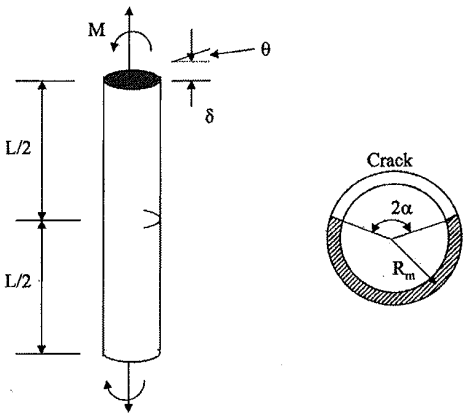

Fig. 2 Analysis of displacement and rotation

If we introduce a crack extension $d\alpha$ (see Fig. 2), we have

$$\frac{\partial U}{\partial \alpha} = \frac{1}{2}[N \quad M] \begin{pmatrix} \dfrac{\partial \delta_c}{\partial \alpha} \\ \dfrac{\partial \theta_c}{\partial \alpha} \end{pmatrix} \tag{5}$$

On the other hand, from the relation between stress intensity factor and strain energy release rate under plane stress condition follows that:

$$\frac{1}{R_m t} \frac{\partial U}{\partial \alpha} = \frac{K_I^2}{E} \tag{6}$$

Here K_I is the stress intensity factor solution for the problem shown in Fig. 2 and R_m and t are the mean radius and thickness of the tube, respectively. The solution is available from Anderson [6], and reprinted in Appendix A of the present paper. It can be written in matrix form as follows:

$$K_I = \begin{bmatrix} \dfrac{\partial K}{\partial N} & \dfrac{\partial K}{\partial M} \end{bmatrix} \begin{pmatrix} N \\ M \end{pmatrix} \tag{7}$$

The energy change, Eq. (6) can be rewritten as

$$\frac{\partial U}{\partial \alpha} = \frac{R_m t}{E}[N \quad M] \begin{bmatrix} \left(\dfrac{\partial K}{\partial N}\right)^2 & \left(\dfrac{\partial K}{\partial N}\right)\left(\dfrac{\partial K}{\partial M}\right) \\ \left(\dfrac{\partial K}{\partial M}\right)\left(\dfrac{\partial K}{\partial N}\right) & \left(\dfrac{\partial K}{\partial M}\right)^2 \end{bmatrix} \begin{pmatrix} N \\ M \end{pmatrix} \tag{8}$$

Comparing Eqs. (5) and (8) gives

$$\begin{pmatrix} \dfrac{\partial \delta_c}{\partial \alpha} \\ \dfrac{\partial \theta_c}{\partial \alpha} \end{pmatrix} = \frac{2R_m t}{E} \begin{bmatrix} \left(\dfrac{\partial K}{\partial N}\right)^2 & \left(\dfrac{\partial K}{\partial N}\right)\left(\dfrac{\partial K}{\partial M}\right) \\ \left(\dfrac{\partial K}{\partial M}\right)\left(\dfrac{\partial K}{\partial N}\right) & \left(\dfrac{\partial K}{\partial M}\right)^2 \end{bmatrix} \begin{pmatrix} N \\ M \end{pmatrix} \tag{9}$$

Now integrating with respect to α gives

$$\begin{pmatrix} \delta_c \\ \theta_c \end{pmatrix} = \begin{bmatrix} \displaystyle\int_0^\alpha \frac{2R_m t}{E}\left(\frac{\partial K}{\partial N}\right)^2 d\alpha & \displaystyle\int_0^\alpha \frac{2R_m t}{E}\left(\frac{\partial K}{\partial N}\right)\left(\frac{\partial K}{\partial M}\right) d\alpha \\ \displaystyle\int_0^\alpha \frac{2R_m t}{E}\left(\frac{\partial K}{\partial M}\right)\left(\frac{\partial K}{\partial N}\right) d\alpha & \displaystyle\int_0^\alpha \frac{2R_m t}{E}\left(\frac{\partial K}{\partial M}\right)^2 d\alpha \end{bmatrix} \times \begin{pmatrix} N \\ M \end{pmatrix} \tag{10}$$

or

$$\begin{pmatrix} \delta_c \\ \theta_c \end{pmatrix} = \begin{bmatrix} C_{11} & C_{12} \\ C_{21} & C_{22} \end{bmatrix} \begin{pmatrix} N \\ M \end{pmatrix} \tag{11}$$

Combining Eqs. (2), (3), and (10), the total displacement and rotation are

$$\begin{pmatrix} \delta_{\text{total}} \\ \theta_{\text{total}} \end{pmatrix} = \begin{bmatrix} L/EA & 0 \\ 0 & L/EI \end{bmatrix} \begin{pmatrix} N \\ M \end{pmatrix} + \begin{bmatrix} C_{11} & C_{12} \\ C_{21} & C_{22} \end{bmatrix} \begin{pmatrix} N \\ M \end{pmatrix} \tag{12}$$

Equation (12) gives the relationship of the external force and moment to the displacement δ and rotation θ at the support of the cracked tube.

For a given circumferential crack geometry, and given tube axial tensile stress (or tensile force N), the reaction bending moment M can be calculated based on the compatibility condition at the supports.

Membrane and Bending Stress in the Tubes. For a given tube area A, and tensile tube stress σ_t, the corresponding tensile force N is calculated from

$$N = A\sigma_t \tag{13}$$

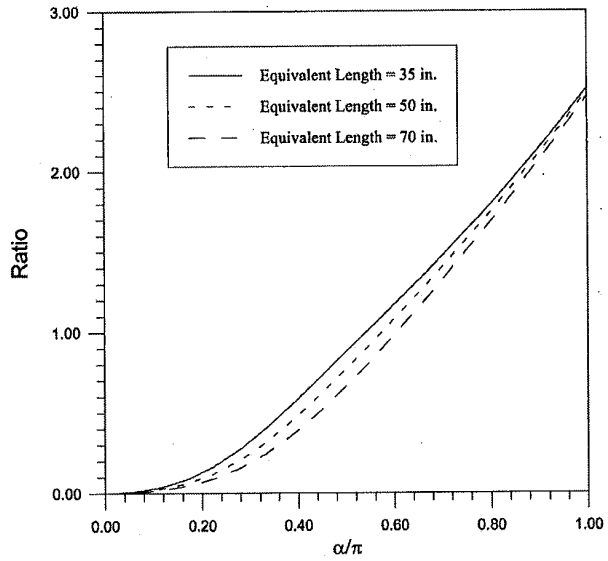

Fig. 3 Crack length versus bending stress σ_b to tensile stress σ_t ratio (σ_b/σ_t)

Then the bending moment M can be obtained by imposing the zero rotation condition at the equivalent cantilever length by applying Eq. (12). In Eq. (12), the axial tube force generates a crack opening moment through C_{21}. The support moment is determined by the compliances of tube and crack, and counteracts the opening moment. Note that the C_{11}, C_{12}, C_{21}, C_{22} are calculated from Eq. (10). The resulting bending moment M is

$$M=-\left(\frac{C_{21}}{\frac{L}{EI}+C_{22}}\right)\cdot N \tag{14}$$

where L is the equivalent cantilever beam length derived in Section 2. The bending moment is then used to calculate the bending stress σ_b

$$\sigma_b=\frac{MR}{I} \tag{15}$$

The foregoing analysis can be conducted easily using any numerical integration scheme. In the current research, Mathcad [7] is used to carry out the analysis for a range of crack dimensions. The typical dimensions used for the tube are

Tube outer diameter: $2R=0.625$ in.

Tube wall thickness: $t=0.038$ in.

Three different values of support plate span are considered:

Length of the support plate span:

$L_{\text{real}}=22.15, 31.65, 44.30$ in

Equivalent cantilever beam length:

$L=35.0, 50.0, 70.0$ in

The tube material is SB-163 UNS N06690. The material properties are from references [2] and [8].

Elastic modulus: $E=30.6\cdot 10^6$ psi

Poisson's ratio: $\nu=0.289$

For three different tube support spans, the resulting ratio between the tensile stress σ_t and bending stress σ_b for different crack lengths α is obtained and plotted in Fig. 3. From these curves, for a given support span value and crack size, the bending stress for any level of tensile stress can be obtained. The resulting tensile stress σ_t and bending stress σ_b can be substituted into Eq. (7) to calculate the stress intensity factor for tubes with support plate of corresponding span.

4 The Limit Load Solution

In this section, the limit load solutions for tubes with a circumferential through-wall crack are discussed. Analytical solutions for tubes without tube support and finite element solutions for tubes with tube support are presented.

Analytical Limit Load Solutions. Two limiting assumptions can be made about the failure of the cracked tube, namely either that it fails purely due to membrane stress, or that it fails only due to bending. These two limiting assumptions can be combined to give a lower-bound limit load.

The limit load for the case where failure occurs due to membrane stress depends linearly on the degraded area through

$$\frac{F_{\text{ax}}}{\sigma_f A}=1-\beta \tag{16}$$

and

$$\beta=\frac{A_{\text{crack}}}{A}=\frac{\alpha}{\pi} \tag{17}$$

where F_{ax} is the limit axial force, σ_f is the flow stress and A is the cross-sectional area of the uncracked tube. The cracked area A_{crack} is proportional to the angular length of the crack, α (Fig. 2). The fraction of degraded area is denoted by β. The percentage of β is also called PDA (percentage degraded area). Failure in membrane of the present crack could occur if the tube is restrained such that no rotation of the tube can occur at the crack location (rigidly held tube).

For the second limiting case, the membrane contribution to failure is neglected, and collapse by pure bending is assumed. A bending moment is caused by the unsymmetrical location of the crack, which moves the neutral axis towards the uncracked side of the tube. The amount x_s by which the neutral axis moves at the cracked section can be found to be

$$x_s=\frac{2}{3}\frac{r_o^2+r_o r_i+r_i^2}{r_o+r_i}\frac{\sin\alpha}{\pi-\alpha} \tag{18}$$

where $r_o=R$ is the outer and r_i is the inner radius of the tube. The moment generated by the applied axial force is $M_{\text{app}}=F_{\text{ax}}x_s$. At the limit state, this moment equals the plastic hinge moment. The resulting equation can be solved for the dimensionless axial force at collapse to give

$$\frac{F_{ax}}{\sigma_f A}=\frac{4}{3}\frac{\sqrt{(r_o^2-x_s^2)^3}-\langle\sqrt{(r_i^2-x_s^2)^3}\rangle}{x_s A}-\frac{A_m}{A} \tag{19}$$

and

$$A_m=\frac{\pi}{2}[r_o^2-\langle r_i^2\rangle]-\left[r_o^2\arcsin\frac{x_s}{r_o}-\left\langle r_i^2\arcsin\frac{x_s}{r_i}\right\rangle\right] \tag{20}$$

where the contents of the $\langle\ \rangle$ brackets is zero if $x_s>r_i$. For short cracks when α is small, (19) gives a higher limit load than (16) because the moment arm x_s is small. On the other hand, above a PDA of about 30%, the bending case becomes the more restrictive one. However, for this failure mode to prevail, the tube must be completely free to rotate (unrestrained) to allow the cracked area a limit failure in bending.

An expression for the lower bound limit load for a combined membrane and bending failure of an unrestrained tube is given by Anderson [6]. Solved for the dimensionless axial force $F_{\text{ax}}/(\sigma_f A)$, the lower-bound limit load is

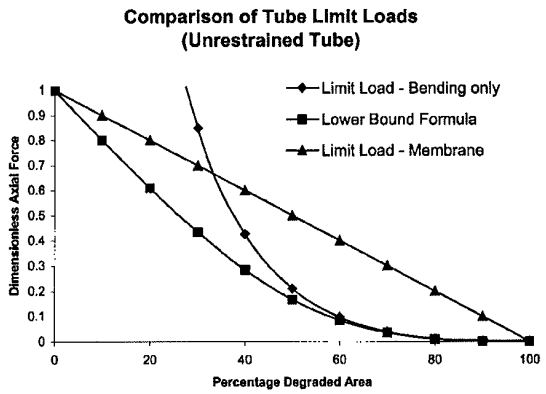

Fig. 4 Comparison of tube limit loads (unrestrained tubes)

$$\frac{F_{ax}}{\sigma_f A} = 1 - \frac{\alpha}{\pi} - \frac{2}{\pi}\arcsin\left(\frac{1}{2}\sin\alpha\right) \tag{21}$$

This formula describes the plastic collapse of a tube that is completely unrestrained against rotations. The failure mode of this tube is combined membrane and bending (as opposed to (19) which describes only the bending contribution). The limit loads from (16), (19), and (21) are compared in Fig. 4. It can be seen how the lower bound formula (21) bounds both (16) and (19), and how the membrane mode and the bending mode dominate for lower and higher PDA, respectively.

Finite Element Solution. The finite element method is used to calculate the limit load for a supported tube. A three-dimensional finite element model [9] of a half-tube was created using 8-noded shell elements. The same tube dimensions as in Section 2 are used. Note that elastic-perfectly plastic properties have been assumed with a flow stress of 55.75 ksi.

The crack was modeled by deleting a row of elements at one end of the model up to the desired angular location. The model is shown in Fig. 5.

The model has symmetry displacement boundary conditions applied on the axial section surface and on the crack ligament (cross-sectional) surface. The cross-sectional surface at the other end of the tube is restrained against radial and circumferential displacements. The nodes are coupled to prevent any bending deflection of the tube, but to allow axial displacements. The uniformly distributed axial end force is applied to the same surface. The boundary conditions are indicated in Fig. 5. The boundary conditions represent two pieces of catilevered tube of 35, 50, 75 in. length each with a midspan crack.

The finite element model described here was analyzed with a PDA of 10 to 90% in steps of 10%. Due to very high strains in the element at the "crack tip," convergence problems were occasionally encountered, and the convergence tolerance for the force was increased to 1.5% in some runs. Therefore, the limit load results do not all fall on a smooth curve.

The results are depicted in Fig. 6. As expected, the results lie between the limiting curves given by Eqs. (16) and (21). For cracks up to 30% PDA, the limit load follows Eq. (21) fairly closely, while for larger PDA, the limit load approaches the membrane failure curve, Eq. (16). Note that detailed finite element analysis indicates that the results for three different equivalent cantilever lengths (35, 50, and 75 in.) are within 1% to each other; therefore, only the results for 50 in. length is plotted and it is applicable for any span range from 35 to 70 in. This new curve will be used as the limit load solution for the cracked tubes with tube support plates in the next section.

5 Failure Assessment of Cracked Tube

Based on the stress intensity factor solutions and limit load solutions presented in Sections 2 and 3, the failure assessment of circumferential cracked tube with tube support is conducted. In the present analysis, the failure assessment diagram approach of Level 3 of PD6493 is used [10]. The assessment for a through-

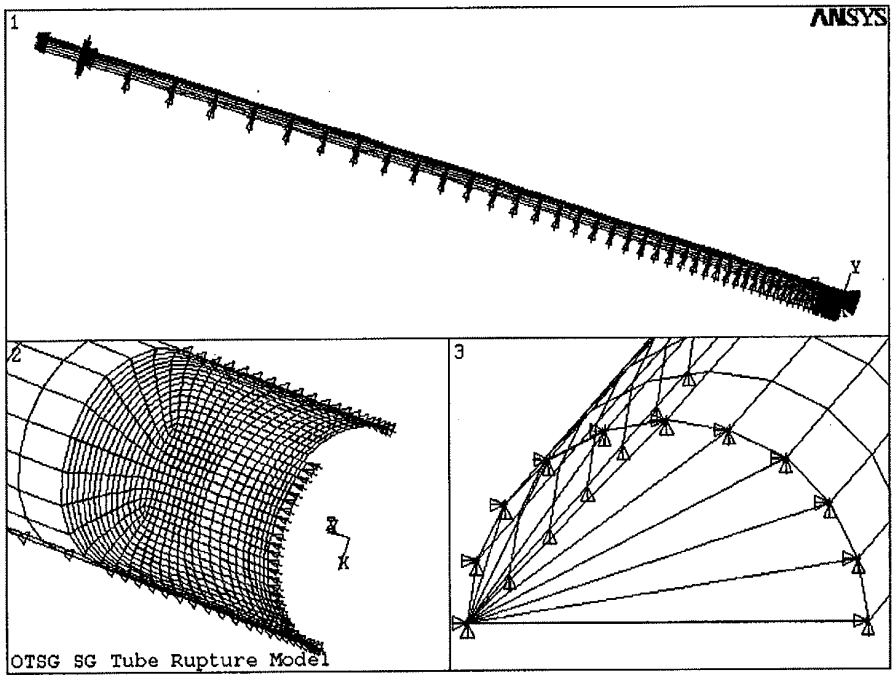

Fig. 5 The finite element model of the tube with tube support

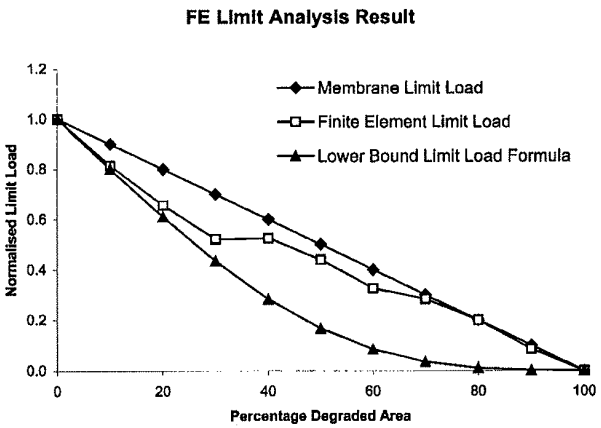

Fig. 6 Finite element limit load analysis results

wall circumferential crack in the SG tube with tube support span value of $L_{real}=31.65$ in or equivalent cantilever span $L=50$ in. is conducted here.

The assessment of the potential of failure is determined by the distance from the origin of the failure assessment diagram (FAD) to the calculated assessment point (K_r, L_r) determined from

$$K_r=\frac{K_I}{K_{IC}} \tag{22}$$

and

$$L_r=\frac{\sigma}{\sigma_L} \tag{23}$$

divided by the distance from the origin to the failure assessment curve. Note that K_r is the stress intensity ratio with K_I being the stress intensity factor for the crack and K_{IC} the toughness of the material. The parameter L_r is the stress ratio, which is the ratio of the applied stress to the limit stress solution calculated based on the yield stress.

In PD6493 [10], a lower bound FAD curve that is independent of geometry and the material stress-strain curve is given by

$$K_r=(1-0.14L_r^2)[0.3+0.7\exp(-0.65L_r^6)] \tag{24}$$

Since the load ratio is defined in terms of the yield strength, L_r can be greater than 1. The typical cut-off is 1.2 for C-Mn steel and 1.8 for austentic stainless steel [10]. In the current analysis, since the flow stress is known for the material used, the ratio of flow stress to the yield stress, σ_f/σ_y is used as the cut-off. Figure 7 shows a plot of the failure assessment diagram.

For the assessment, a range of stresses is applied which corresponds to different operating conditions of the steam generator. The maximum crack size for each loading condition, represented by PDA (percentage degraded area), is obtained from the failure assessment diagram. The axial stress is normalized as follows:

$$P_n=\frac{\sigma}{\sigma_f} \tag{25}$$

where σ_f is the flow stress of the material equals $0.5(\sigma_y+\sigma_u)$, with σ_y and σ_u yield and ultimate strengths, respectively. The yield strength and ultimate strength of Alloy 690 are taken at 650°F, where they equal 31.5 ksi and 80 ksi, respectively [2,8]. Therefore, the cut-off in the FAD is $55.75/31.5=1.77$. The fracture toughness K_{IC} is obtained by converting a J_{IC} value. The J_{IC} value used is 571 in-lb/in^2 based on a conservative estimation.

The resulting maximum PDAs for a normalized axial stress are presented in Fig. 8. As a comparison, the PDA results for tubes without tube support are also shown. It can be observed that it is

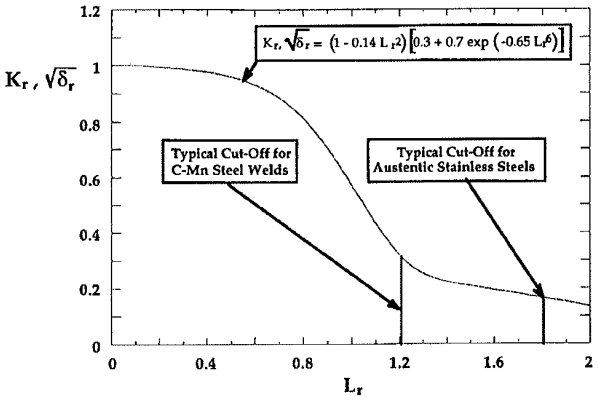

Fig. 7 Failure assessment diagram Level 3 of PD: 6493 [10]

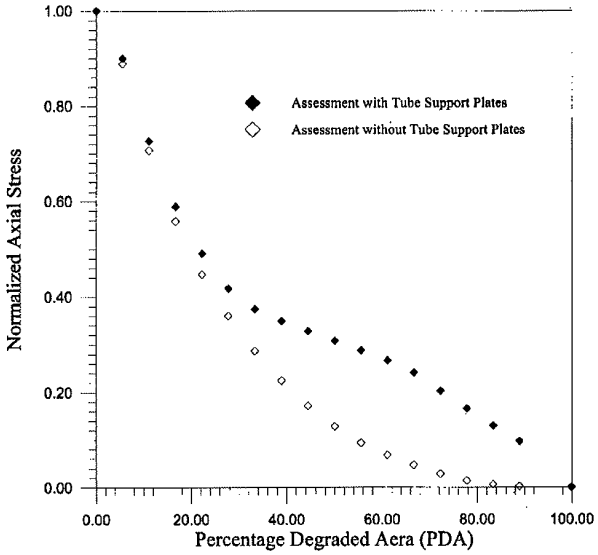

Fig. 8 Results from the failure assessment, span L_{real} =31.65 in.

overly conservative to exclude the effect of the tube supports. By accounting for the effect of the tube support plates, the increase in the allowable PDA can be as much as 20 to 30% in the present example.

6 Conclusions

The stress intensity factors and limit loads are presented for tubes with circumferential through-wall cracks when taking the restraining effect of the tube support plates into account. Based on the presented solutions, the assessment of typical steam generator tube with through-wall circumferential cracks of various sizes is conducted. It is demonstrated that the maximum allowable PDA can increase by as much as 20 to 30% compared to an assessment that does not consider the restraint of the tube support plates.

Acknowledgments

Part of the research reported here was conducted when one of the authors (XW) was with Nuclear Engineering, Babcock and Wilcox Canada. Support from Mr. N. Idvorian is gratefully acknowledged. Financial support to XW from Natural Sciences and Engineering Research Council of Canada (NSERC) is also gratefully acknowledged.

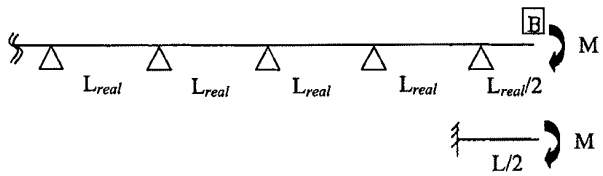

Fig. 9 Periodically supported beam and equivalent cantilever

Appendix A

Stress Intensity Factor Solutions for Partial Through-Wall Circumferential Cracks. From Anderson [6] the stress intensity factor for the problem described in Fig. 2 is written as

$$K_I = \left[\frac{\partial K}{\partial N}\ \frac{\partial K}{\partial M}\right]\begin{pmatrix} N \\ M \end{pmatrix}$$

where

$$\frac{\partial K}{\partial N} = \left[1 + A\left[5.3303 \cdot \left(\frac{\alpha}{\pi}\right)^{1.5} + 18.773 \cdot \left(\frac{\alpha}{\pi}\right)^{4.24}\right]\right] \cdot \frac{\sqrt{\pi R\alpha}}{2\pi Rt}$$

$$\frac{\partial K}{\partial M} = \left[1 + A\left[4.5967 \cdot \left(\frac{\alpha}{\pi}\right)^{1.5} + 2.6422 \cdot \left(\frac{\alpha}{\pi}\right)^{4.24}\right]\right] \cdot \frac{\sqrt{\pi R\alpha}}{R^2 t}$$

$$\text{and} \quad A = \left(0.125 \cdot \frac{R}{t} - 0.25\right)^{0.25} \qquad \text{for} \quad 5 \leq \frac{R}{t} \leq 10$$

Appendix B

Derivation of a Cantilever Beam Length Equivalent in Stiffness to an Infinite Periodically Supported Tube. Consider a semi-infinite beam with evenly spaced (distance L_{real}) supports, ending in a cantilever of $L_{\text{real}}/2$ as shown in the Fig. 9. The objective is to find the equivalent length L of a simple cantilever beam such that an applied moment M causes the same rotation θ as at the end point B of the semi-infinite beam.

First, consider a cantilevered beam of length $L_{\text{real}}/2$ with simple support and a torsional spring of stiffness C_0 at one end. Given the moment of area I and Young's modulus E, the end rotation θ is [11]

$$\theta\left(\frac{L_{\text{real}}}{2}\right) = \frac{ML_{\text{real}}}{2EI} + \frac{M}{C_0} \tag{26}$$

The rotational stiffness C_0 is caused by the semi-infinite simply supported beam that is loaded by a moment on the last support. In this situation, a single simply supported beam of length L_{real} has the stiffness [11]

$$C_{B1} = \frac{3EI}{L_{\text{real}}} \tag{27}$$

If this single beam is attached to another identical beam, the next beam imposes a moment on the other end of the beam, and the effective stiffness increases. The same is true if another beam is added to this structure, and so on. The rotational stiffness of an n-beam structure can be expressed in terms of the stiffness of the n-1 beam structure that is attached to a single simply supported beam through

$$C_{Bn} = C_{B1}\frac{1 + \dfrac{C_{Bn-1}}{C_{B1}}}{1 + \dfrac{3}{4}\dfrac{C_{Bn-1}}{C_{B1}}} \tag{28}$$

This recursion formula converges quickly to a stationary value that is assumed when $n \to \infty$. By using the condition $C_{B\,n} = C_{B\,n-1}$ in (28), it can be shown that

$$C_{B\infty} = \frac{2\sqrt{3}}{3} C_{B1} \tag{29}$$

Going back to the initial cantilever portion of the infinite beam, one can now substitute $C_0 = C_{B\infty}$ into (26) to obtain

$$\theta\left(\frac{L_{\text{real}}}{2}\right) = \frac{ML_{\text{real}}}{2EI}\left(1 + \frac{\sqrt{3}}{3}\right) \tag{30}$$

Now using the simple cantilever beam with length L, the required equivalent length L is found to be

$$L = L_{\text{real}}\left(1 + \frac{\sqrt{3}}{3}\right) = 1.58L_{\text{real}} \tag{31}$$

Therefore, the required length L in the model is $1.58L_{\text{real}}$.

References

[1] NRC Regulatory Guide 1.121, 1976, "Bases for Plugging Degraded PWD Steam Generator Tubes," U.S. Nuclear Regulatory Commission, Aug.

[2] ASME Boiler & Pressure Vessel Code, 1998 Edition, Section III and XI, including Appendices.

[3] Bloom, J., 1985, "Deformation Plasticity Failure Assessment Diagram," Elastic-Plastic Fracture Mechanics Technology, ASTM Spec. Tech. Publ., ASTM STP 896.

[4] EPRI TR-107197-P1 & P2, Interim Report, 1997, "Depth-Based Structural Analysis Methods for Steam Generator Circumferential Indications," Nov.

[5] Marchand, N., Parks, D.M. and Pelloux, R.M. 1986, "K_I Solutions for Single Edge Notch Specimens under Fixed End Displacement," Int. J. Fract., **31**, pp. 53–65.

[6] Anderson, T. L., 1995, *Fracture Mechanics, Fundamentals and Applications*, Second Edition, CRC Press Inc., Boca Raton, FL.

[7] Mathcad 6.0, 1995, User's Manual, MatSoft Inc.

[8] Huntington Alloys, 1980, "Inconel Alloy 690," Huntington Alloys, Inc.

[9] ANSYS Release 5.6, 1999, User's Manual, 11th Edition, ANSYS Inc.

[10] PD 6493:1991, 1991, "Guidance on Some Methods for the Derivation of Acceptance Levels for Defects in Fusion Welded Joints," British Standards Institution, Aug.

[11] Young, W. C., 1989, *Roark's Formulas for Stress and Strain*, 6th Edition, McGraw-Hill Inc., New York. NY.